CANADA

DEPARTMENT OF
ENERGY, MINES AND RESOURCES
MINES BRANCH
OTTAWA

THE RISING-LOAD CANTILEVER TEST: A RAPID TEST FOR DETERMINING THE RESISTANCE OF HIGH-STRENGTH MATERIALS TO ENVIRONMENTAL CRACKING

B. C. SYRETT AND G. J. BIEFER

PHYSICAL METALLURGY DIVISION

JULY 1970

Research Report R 227

Price $1.00

Available by mail from Information Canada, Ottawa
and at the following Information Canada bookshops

HALIFAX
1735 Barrington Street

MONTREAL
Æterna-Vie Building, 1182 St. Catherine St. West

OTTAWA
171 Slater Street

TORONTO
221 Yonge Street

WINNIPEG
Mall Center Bldg., 499 Portage Avenue

VANCOUVER
657 Granville Street

or through your bookseller

Price $1.00 Catalogue No. M 38-1/227

Price subject to change without notice

Information Canada
Ottawa, 1971

Mines Branch Research Report R 227

THE RISING-LOAD CANTILEVER TEST: A RAPID TEST FOR DETERMINING THE RESISTANCE OF HIGH-STRENGTH MATERIALS TO ENVIRONMENTAL CRACKING

by

B.C. Syrett* and G.J. Biefer**

- - - - - - - -

ABSTRACT

The cantilever test, first reported in 1965 by B.F. Brown and co-workers at the U.S. Naval Research Laboratory, Washington, D.C., has been used in environmental-cracking (EC) tests in which the specimen load is increased at a uniform rate until failure occurs. Tests on 18% Ni (250) maraging steel in 3.5% NaCl solution have shown that the nominal stress intensity at fracture, K_{Ii}^{*}, is a convenient measure of susceptibility to EC, provided that the loading rate is 10 psi$\sqrt{\text{in.}}$/min or less. For specimens cut from 0.5-in. plate, rising-load tests performed at 5-10 psi$\sqrt{\text{in.}}$/min took 0.5 to 1 week, but were economical of both metal specimens and technician working time, as compared with constant-load tests. It is considered that the procedures developed should provide a suitable routine screening test for estimating the EC susceptibilities of

*Research Scientist and **Head, Corrosion Section, Physical Metallurgy Division, Mines Branch, Department of Energy, Mines and Resources, Ottawa, Canada.

other high-strength materials.

Results from the rising-load cantilever test indicate that 18% Ni (250) maraging steel, in the presence of a sharp notch, is highly susceptible to EC when cathodically protected at or near the potential provided by zinc (i.e., about -1060 mV SCE). Maximum resistance to EC was observed in the rather narrow potential range of -700 to -750 mV.

Results from the rising-load cantilever tests are compared with constant-load cantilever tests and constant-load tests conducted on smooth cylindrical specimens axially loaded. The shortcomings of the latter test method are discussed.

Direction des mines

Rapport de recherches R 227

L'ESSAI CANTILEVER À CHARGE CROISSANTE: UN MOYEN RAPIDE DE DÉTERMINER LA RÉSISTANCE À LA FISSURATION ENVIRONNEMENTALE DES MATÉRIAUX À GRANDE RÉSISTANCE

par

B. C. Syrett* et G. J. Biefer**

RÉSUMÉ

L'essai cantilever premièrement rapporté en 1965 par B. F. Brown et ses collaborateurs du U. S. Naval Research Laboratory, à Washington (D. C.), a été utilisé pour des essais de fissuration environnementale dans lesquels la charge exercée sur l'éprouvette est accrue jusqu'à la rupture. Les essais effectués sur des éprouvettes d'acier "maraging" (250) à 18 p. 100 de Ni dans une solution contenant 3. 5 p. 100 de NaCl ont montré que la tension nominale à la rupture, K^*_{Ii}, est une mesure commode de la susceptibilité à la fissuration environnementale, pourvu que le taux de chargement soit égal ou inférieur à 10 lb/po^2 $\sqrt{\text{po}}$/min. Dans le cas d'éprouvettes prélevées dans une plaque d'un demi-pouce, les essais de chargement graduel exécutés à un rythme de 5 à 10 lb/po^2 $\sqrt{\text{po}}$/min. ont duré d'une demi-semaine à une semaine mais se sont avérés économiques en ce qui a trait au nombre des éprouvettes et au temps de travail des techniciens comparativement aux essais à charge constante. Les auteurs estiment que les méthodes élaborées devraient constituer un bon essai de routine pour l'évaluation de la susceptibilité à la fissuration environnementale

---

* Chercheur scientifique et **Chef, Section de la corrosion, Division de la métallurgie physique, Direction des mines, ministère de l'Énergie des Mines et des Ressources, Ottawa, Canada.

d'autres matériaux à grande résistance.

Les résultats de l'essai cantilever à charge croissante indiquent que l'acier "maraging" (250) à 18 p. 100 de Ni, lorsque l'entaille de l'éprouvette est aiguë, est très susceptible à la fissuration environnementale lorsqu'une protection cathodique est assurée environ au potentiel fourni par le zinc (c'est-à-dire, d'environ -1060 mV par rapport à une électrode de calomel saturée). La résistance maximale à la fissuration environnementale a été observée dans la gamme de potentiel plutôt étroite de -700 à -750 mV.

Les auteurs comparent les résultats des essais cantilever à charge croissante avec ceux des essais cantilever à charge constante et des essais à charge constante exécutés sur des éprouvettes cylindriques lisses chargées axialement. Ils discutent enfin les lacunes de cette dernière méthode d'essai.

CONTENTS

= = =

TABLES

FIGURES

Page

▪ = = ▪

INTRODUCTION

Since the beginning of this century, there has been an increasing awareness that the premature failure of a metal by cracking may be induced by the conjoint effects of corrosion and a static tensile stress. The term "stress-corrosion cracking" (SCC) has long been used to describe this phenomenon in low- and medium-strength materials. SCC will not occur if either the stress or the corrosive environment is absent; cracks initiate and propagate by selective dissolution at anodic sites on the metal surface until final rupture by mechanical overload occurs.

With the development of new high-strength steels and titanium alloys during the past decade, it has become increasingly evident that environmentally induced cracking of stressed metals may occur in many aqueous solutions as a result of a second process, namely "hydrogen embrittlement cracking" (HEC). Whereas SCC, as originally defined, is strictly a deterioration of the metal at anodic sites, HEC occurs as a consequence of cathodic reduction of hydrogen from the electrolyte and its absorption by the metal at these cathodic sites. Although the exact mechanism is debated, a deleterious interaction between hydrogen and the metal lattice allows slow crack growth, and premature failure of the metal. Under some circumstances it may not be clear which process is responsible for cracking, and in others, both SCC and HEC may each take a part in the overall cracking process: it is useful, therefore, to define a general term which includes

both SCC and HEC. Many workers use "stress corrosion" as this general term, but understandably this has led to some confusion amongst people whose main interests lie outside this field. Of the other suggestions which have been made, the term "environmental cracking" (EC) appears to best convey the essential idea of slow crack growth in a corrosive environment.

A study of EC in low-strength materials is normally performed on smooth specimens, although in special cases notched specimens have been used. In high-strength materials the converse is true, and though the more conventional smooth specimens have been usefully employed in some tests, the susceptibility to EC is usually more clearly demonstrated with specimens which contain sharp precracks prior to testing. These precracks are normally formed at the root of a notch, slot, or hole in the metal by a low-stress fatiguing operation. Details of the proportions of nine specimens in current use are given in a recent review [1]. When smooth specimens are used, it is frequently found that a prerequisite to crack propagation is the formation of a surface pit, which then acts as a local stress raiser to promote cracking from its base. The time required to form a pit is often a large proportion of the total testing time, and, in the case of certain titanium alloys, the pits may never form. Thus, one of the advantages of using a precracked specimen is that the resistance of a metal to crack propagation may be studied in a relatively short testing period; also, the EC susceptibility of a metal which is resistant to pitting may be assessed without difficulty.

Having once decided to use specimens with a built-in flaw, it is necessary to determine whether the nominal stress at the tip of the precrack

is the most meaningful parameter to relate to EC susceptibility. In fact, it has been demonstrated that the stress conditions existing at the precrack tip are best characterized by a fracture mechanics parameter, called the stress intensity factor, "K", which is proportional to the product of the nominal stress and the square root of the crack size. Equations have been calculated which relate K to the applied load and the crack size for a number of different specimen shapes (for example, see reference 1).

By measuring K, instead of nominal stress, the results collected are effectively independent of specimen shape, and the probable behaviour of service components can,in some instances, be accurately predicted. Smith et al.[2] provided very strong evidence that the stress-intensity parameter is of prime importance, when they arranged that the loading method and shape of their titanium alloy specimens were such that, at constant load, K first decreased with increasing environmental crack length, before passing through a minimum and rising again. The nominal stress, on the other hand, increased continuously as the crack grew. When the applied load was low, their data showed that, as K diminished, the crack propagation rate decreased to a point of apparent arrest, despite the rising net-section stress.

When a precracked specimen is loaded in an inert atmosphere, the stress intensity may be increased by increasing the applied load, but eventually a critical stress intensity, K_c, is exceeded and unstable "fast fracture" will occur. K_c, often called the "fracture toughness" of the material, initially decreases with increasing specimen thickness; a thickness

is reached, however, where plane-strain [+] conditions prevail over the greater part of the crack front, and for specimens with this or greater thickness, the fracture toughness has its minimum value, K_{Ic}, described as the "plane-strain fracture toughness". The Roman numeral I in the subscript of K_{Ic}, though it has been adopted to denote plane-strain conditions too, primarily indicates that the crack grows in the tensile opening mode, as opposed to the sliding modes, II and III.

During an EC test, the stress intensity may increase either because the applied load is increased or because the crack size increases, but eventually the stress intensity for terminal fast fracture is reached, termed $K_{I\delta}$. Some workers [3] have found that $K_{I\delta}$ is equal to K_{Ic}, but others [4] point out that where EC causes crack blunting, $K_{I\delta}$ may exceed twice this value. The equations commonly used to calculate $K_{I\delta}$ and K_{Ic} are only truly valid, of course, for a sharp crack.

Of the many EC testing methods available, the cantilever test developed by Brown and Beachem at the U.S. Naval Research Laboratories [3] is perhaps one of the most convenient. Here, a notched bar, precracked at the notch root by fatiguing, is loaded as a cantilever beam. The test solution, which surrounds the precracked region of the bar, is contained in a plastic vessel. The EC properties of a metal are assessed by setting a number of specimens in the corrodent at various initial stress intensities

---

[+] A complete definition of the term "plane strain" is outside the scope of this report; suffice it to say that in any of the specimens in common use (i.e., with the precrack perpendicular to the applied load), fast fracture will occur in the plane of the precrack when plane-strain conditions prevail.

and observing the cracking behaviour. Brown and Beachem plotted the initial stress intensity, K_{Ii}, as a function of time-to-failure, and the minimum value of K_{Ii} which was observed to cause SCC was designated K_{ISCC}. This term is now defined [1] to denote applicability to both SCC and HEC, and is widely accepted as an EC parameter which is characteristic of a particular alloy in a selected heat treatment condition.

Determination of K_{ISCC} is not in itself sufficient to describe the resistance of a metal to EC, because it gives no indication of crack incubation times or propagation rates. A metal component with a low K_{ISCC} value might give adequate service when used at fairly high stress-intensity levels, if the rate of crack propagation is very low. A complete K_{Ii} versus time-to-failure curve would certainly provide all the necessary information, but in some circumstances it might not be practical to obtain the necessary data points, because of such factors as insufficient material, limited machine-shop facilities, or lack of technical assistance. Because these considerations were of some importance in early work [5] performed in this laboratory, each specimen was loaded in stages, the time at each stress intensity level varying from 1 to 68 hours. The numerous data points provided by each specimen were then plotted on stress-intensity vs time-to-failure curves. Although general trends in EC behaviour could certainly be determined using this testing procedure, it was recognized that the loading of the cantilever beam by manual addition of weights was both awkward and time-consuming. Furthermore, although it became clear that the loading rate often had a great influence on the nominal stress intensity at fracture, the use of

incremental loading left this rate, at best, roughly defined. It was decided, therefore, to develop equipment and experimental techniques such that routine screening tests could be performed rapidly, and under controlled conditions, to estimate the relative susceptibilities of high-strength materials to EC.

The EC behaviour of 18% Ni (250) maraging steel was considered to be of particular importance, because this material is being used in the foils system of the Canadian FHE-400 hydrofoil craft. Thus, all measurements were carried out on this steel.

Because a number of workers have investigated the EC behaviour of high-strength steels by means of tests on axially-loaded, smooth specimens of circular cross-section, it was decided to carry out some measurements of this type also, using a "Unisteel" testing machine.

EXPERIMENTAL

Testing Equipment

Two types of cantilever testing rig were used: one similar to that used previously [5], constructed according to shop drawings supplied by B.F. Brown of the U.S. Naval Research Laboratories, Washington, D.C., and another, more automated rig which was designed to facilitate precise control over the experimental conditions. The former can be made quickly and cheaply from 6061-T6 aluminum stock, and may be adequate for occasional use, e.g., in small-scale development testing. When EC tests are to be performed on a more regular basis, or as part of a research

program where testing conditions must be carefully controlled, the advantages of the automated rig would soon become apparent. The specimen-clamps and beam of the automated rig are machined from Type 431 stainless steel, heat treated to 130,000 psi yield strength, and the vertical support and base is an all-welded mild steel structure.

Materials and Specimen Size

Specimens were cut from four 0.5-in.-thick 18% Ni maraging steel plates of nominally the same composition. The heat treatment and other details of these maraging steels are given in Table 1. Both cantilever and Unisteel specimens were cut from two of the plates, only Unisteel specimens were taken from another, and three separate batches of cantilever specimens were taken from the fourth plate. The chemical compositions of the steels used in this work are given in Table 2, except for the D_u series, for which the exact composition is unavailable.

Figure 1 shows the dimensions of the standard cantilever specimens. They were machined in the solution-annealed condition, heat treated, then precracked at the root of the top-notch by fatiguing in a Krouse reverse-bend plate fatigue testing machine. In order to avoid excessive damage at the tip of the fatigue precrack, a comparatively low stress intensity (about 6.5 ksi$\sqrt{\text{in.}}$)* was applied during the fatiguing operation. Under such conditions, a crack about 0.020 in. deep was developed in 20,000 cycles; occasionally fatigue precracks were produced which were as shallow as 0.013 in. or as deep as 0.050 in. in depth, but some preliminary work suggested that, within this range, the precracking rate had no effect on EC

* ksi, widely used in the U.S.A., is equivalent to kpsi.

properties.

The major axis of the cantilever specimens was in the rolling direction, and the depth (D) corresponds to the short transverse dimension of the original rolled plate. The final depth, after machining, was constant for any one series of specimens, but varied from series to series in the range 0.440 in. to 0.502 in. (see Table 1).

Unless otherwise stated, the thin heat-treatment oxide was not removed from the surface of cantilever specimens prior to the EC tests.

The final dimensions of the Unisteel specimens are shown in Figure 2; however, to maintain dimensional stability during heat treatment, it was found necessary to increase the light section of the gauge length by 0.040 in. Only after heat treatment was the gauge-length diameter reduced by fine grinding to the standard 0.126 in. The major axis of each specimen was in the rolling direction.

The C_u series and some of the D_u series Unisteel specimens contained welded material in the gauge length: prior to machining these specimens, a single plate was cut in half in the plane perpendicular to the rolling direction, and welded together by the tungsten-inert-gas ("TIG") process. Weld-metal specimens were compared with the parent-metal specimens of the B_u series and the rest of the D_u series.

Manually-Loaded Cantilever Testing Rig

Figure 3 shows the cantilever testing rig which was used previously [5]; this rig was used to test B, C, and E series specimens. One end of a specimen was clamped to the vertical support, whilst the other end was clamped

to the cantilever beam. The specimen was stressed by hanging suitable weights from the end of the beam.

During an EC test, the central 2 in. of the specimen was surrounded with 3.5% NaCl solution contained in a plastic corrosion cell. This cell can be made from a polyethylene bottle with its top cut off, and rectangular holes of appropriate size cut through its sides. The joints between the specimen and corrosion cell were sealed externally with either General Electric silicone construction sealant or Lepage's epoxy glue. An enlarged view of this region is shown in Figure 4. A Luggin probe is shown, which leads through a salt bridge to a saturated-KCl calomel electrode, so permitting measurements of specimen potential, during the tests, by means of a Keithley 601 electrometer. Figure 4 also shows the sacrificial anodes of 99.999% Zn which were coupled externally to some E series specimens to provide "cathodic protection". Some B series specimens were cathodically polarized, too, but here the active potentials were obtained by using a Duffer's Model 600 potentiostat. A platinized-platinum auxiliary electrode was used to supply the polarizing current, and a saturated-KCl calomel electrode was used as a reference electrode. These EC tests differed from those of the E series in that B series specimens were given no-load cathodic charging pretreatments of 24 hr prior to the commencement of loading.

The salt solution in the corrosion cell was replaced at a rate of about 4 ℓ/day from the reservoir shown at the top of Figure 3. The replacement rate was controlled by adjusting a screw clip which pinched the plastic

delivery tube and restricted flow; frequent readjustments were needed as the water-level in the reservoir decreased.

The load was increased in increments during the tests. As is shown in Figure 3, weights could be positioned on the holder hanging from the end of the cantilever beam. An automobile jack, fitted with a special platform, was used to remove the stress from the specimens when weights were being added, and it also served as a landing pad for the weights when fracture occurred. The latter action deactivated a timer which was controlled by a microswitch recessed in the landing pad. Unless fracture occurred, each loading level was maintained for a period in the range 1 min to 1 week before going on to the next higher load level. If a specimen had not fractured at the end of a working day, the load was left on overnight; the loading schedule was continued the following morning if fracture still had not occurred. The increment of load added was typically 0.25 lb (equivalent to a K_{Ii} increase of about 0.5 ksi$\sqrt{\text{in.}}$) but was occasionally as high as 2 lb. The loading rate, calculated as the rate of increase in stress intensity, was thus dependent partly on the precrack depth, partly on the load increment, and partly on the time between these increments. Some tests were performed on dry specimens, in the absence of a corrosive environment, and here, too, the loading rate was varied over a fairly wide range.

Automated Cantilever Testing Rig

Figure 5 shows how the simple testing rig described above has been adapted to provide a continuously increasing load test. Here, the loading medium, water, was siphoned from a 20-gallon reservoir, positioned above

the rig, into a plastic loading vessel which hung from the end of the cantilever beam. The upper end of the glass siphon-tube was cemented to a bottom-weighted raft floating on the surface of the water reservoir. The lower end of the siphon was fitted with one of a number of delivery nozzles, the internal diameter of which controlled the rate of siphoning, hence the rate of loading. As water siphoned into the loading-vessel, the raft descended with the reservoir water-level, and since there was no relative movement between the ends of the siphon-tube, the rate of loading remained constant. Uniform rates of loading in the range 0.125 lb/hr to 360 lb/hr have been obtained in this fashion without difficulty, and it seems reasonable to assume that this range could be extended further by judicious choice of siphon-tube and delivery nozzle diameters, and by increasing or decreasing the effective head of water.

It should be noted that in some of the early long-term tests, flow rates tended to decrease gradually because of the build-up of organic growths in the narrow delivery nozzles; this was particularly noticeable when Ottawa tap water, rather than distilled water, was used as the loading medium. It was found that this could be prevented completely by the addition of a suitable germicide to the reservoir water, e.g., 10 ppm Hyamine 3500 (50% concentrate)[+] or 0.01 g/ℓ $CuSO_4$.

In these rising-load tests, the load increased until the stress intensity to cause fast fracture in the specimen was exceeded. At fracture, the drop

[+]Available from Rohm and Haas Company of Canada, Limited, West Hill, Ontario, Canada.

of the loading vessel activated microswitches controlling the electrically-operated water cut-off valve and the timing clocks. The cut-off valve, situated in the siphon-tube line just above the raft, was thus closed at fracture, preventing further siphoning of the water.

Under normal experimental conditions the 3.5% NaCl solution (pH = 6.0 to 6.5) in the corrosion cell was replaced at the rate of 6 ℓ/day by dripping salt solution into the cell at a constant rate, and running an overflow tube to the drain. At this relatively low delivery rate, a constant-flow-rate system was set up, using a much simpler method than the one described above. A large plastic carboy, fitted with a spigot, was used as the salt solution reservoir; the mouth of the carboy was closed with a rubber stopper, fitted with a glass air-inlet tube long enough to reach the bottom of the reservoir (see Figure 5). With the spigot open, the salt solution dripped through a capillary-tube exit into the corrosion cell. The subsequent drop in the reservoir level created a partial vacuum in the space above the salt solution, and eventually air was drawn into the reservoir via the air-inlet tube. Under these conditions, the effective head of the salt solution was always between the bottom of the air-inlet tube (at atmospheric pressure) and the capillary tube exit, so salt solution was supplied at a constant rate. The pressure exerted by the volume of liquid above the air-inlet tube base was exactly balanced by the partial vacuum in the air space. The rate of delivery of the corrodent could be adjusted simply by raising or lowering the capillary-tube exit. This arrangement was clearly superior to that used in the manual loading tests.

In addition to the rising-load tests, a few constant-load ("static") tests were performed on the automated rig. In this type of test, environmental crack propagation was monitored by means of a Daytronic linear variable displacement transducer (LVDT) positioned to measure the deflection of the cantilever beam as cracking proceeded (see Figure 5); the output from the LVDT was fed into a Texas Instruments Servoriter II potentiometric chart recorder. The sensitivity of the LVDT in detecting cracking depended, in part, on the point chosen on the cantilever beam to monitor the deflection. The farther from the test specimen, the larger was the beam displacement for a given crack propagation distance; however, at distances greater than an inch or two from the specimen, a correction had to be made for the loading effect of the LVDT probe.

Figure 6 shows the notched test specimen and the corrosion cell. The joints between the specimen and the plastic corrosion cell were sealed externally with either General Electric silicone construction sealant or Lepage's epoxy glue (not shown in Figure 6).

The electrochemical potential of the freely corroding specimen was measured, with respect to a saturated calomel reference electrode, by means of a Keithley 601 electrometer and recorded, via this high-impedance electrometer, by a Texas Instruments Servoriter II potentiometric chart recorder. The potential could also be controlled, when desired, to within ±1 mV by an Anotrol Model 4700M potentiostat; platinized-platinum auxiliary electrodes were placed on either side of the bar specimen to supply the polarizing current. In one instance, the specimen was coupled to

aluminum alloy 5083 sacrificial anodes which polarized the specimen to an average potential of -782 mV (+11, -19 mV).

E_1 series specimens were used for all rising-load tests on the automated rig, and E_1 and E_2 series specimens were employed for the constant-load tests.

Unisteel Testing Machine

Full details of the operation and design of this machine may be obtained from the manufacturer[+], but a short description is given here. The specimen was loaded through a double lever system (see Figure 7) which, with a 30:1 loading ratio, gave a maximum load of 2800 lb, equivalent to 224 ksi on a standard 0.126-in.-diameter specimen. The specimen was held between top and bottom tension rods, the lower being connected to the lever loading system, and the upper to an adjusting nut arrangement; this nut was adjusted until a spirit level, positioned on the outer lever, indicated that the lever system had been levelled. When a specimen failed, the inner lever deactivated a microswitch which controlled the power supply to a timing clock; thus, the duration of a test was recorded automatically. Rubber washers and locking nuts were used to seal the joint between the bottom of the plastic corrosion cell and the specimen. The nut outside the corrosion cell was made from stainless steel, but a "Teflon" fluorocarbon resin nut was used on the inside so as to eliminate the possibility of galvanic action.

[+] Distington Engineering Company Limited, Workington, Cumberland, England.

In the B_u and C_u series tests, the 3.5% NaCl solution was not replenished, but in the D_u series tests the solution was replenished by gravity feed at a rate of approximately 4 ℓ/day. The salt solution reservoir was supported above the testing machine, as shown in Figure 7.

Stress-Intensity Calculations

In the constant-load cantilever tests, the initial stress intensity, K_{Ii}, was calculated as follows:

$$K_{Ii} = \left(\frac{B}{B_N}\right)^{\frac{1}{2}} \frac{\beta M}{BD^{3/2}} \quad \ldots\ldots\ldots\ldots\ldots\ldots \quad (1)$$

B is the thickness of the bar, B_N is the thickness in the notched plane, D is the width, M is the bending moment at the notch (i.e., beam length x load at end of beam), and β is a function of a/D:

$$\beta = 4.12 \sqrt{\frac{1}{(1-a/D)^3} - (1 - a/D)^3}, \quad \ldots\ldots\ldots \quad (2)$$

where "a" is the precrack depth (notch + fatigue crack). These symbols are marked in Figure 1. The term $\left(\frac{B}{B_N}\right)^{\frac{1}{2}}$ does not appear in the similar equation used by Brown and Beachem [3], and is the correction suggested by Freed and Krafft [6] for the side-notching. A graphical short-cut for obtaining β is presented in Figure 8.

In rising-load cantilever tests, the nominal stress intensity at fracture was designated K^*_{Ii}, the asterisk being used to differentiate it from values of K_{Ii} obtained in constant-load tests. K^*_{Ii} was also calculated, using Equations 1 and 2, from the values of the initial crack depth "a" and the load at fracture.

Rising-load tests were also carried out on dry specimens in order to obtain a base-line stress intensity value; here, K^*_{Ii} approximates K_{Ic} because no slow crack growth occurs during loading[+].

The cantilever beam and the empty loading-vessel were in themselves sufficiently heavy to impart an appreciable stress to the specimen; so, in calculating the loading rate in terms of rate of increase in stress intensity, this initial stress intensity was subtracted from the K^*_{Ii} value before dividing by the testing time.

RESULTS

A study of the EC mechanism in 18% Ni (250) maraging steel has already been published elsewhere [8]. The results of greatest technological significance obtained in this work are consolidated in the present report with previously unpublished data, to facilitate an assessment of the suitability of the rising-load cantilever test as a routine screening test.

[+]The dimensions of the specimens without side-notches, used in this work, did not meet the requirements recommended by the ASTM Committee E-24 [7] for the attainment of plane-strain conditions; thus the K_{Ic} values quoted for these specimens may not be valid plane-strain fracture toughness values. However, the error involved is thought to be small, and the subscript 'I' is retained, if for no other reason than to denote that the crack grows in the tensile-opening mode. By machining side-notches in the specimens, flat fractures in the plane of the precrack and notches (the normal indication of plane-strain conditions) were produced. Thus, K_{Ic} values determined for side-notched specimens were probably quite accurate, assuming the empirical correction for side-notching, $\left(\frac{B}{B_N}\right)^{\frac{1}{2}}$, is accurate.

Effect of Loading Rate on K^*_{Ii} (Cantilever Tests)

Although all the maraging steels were nominally of the same composition, and had been given the same heat treatment, each series possessed its own unique fracture toughness value, K_{Ic}. The mean values of K_{Ic} obtained for the B, C_1, E, E_1 and E_2 series steels are shown in Table 3: the B_u and C_u series were considered to have K_{Ic} values respectively similar to the B and C_1 series steels. It is not clear why such variations in the fracture toughness values occurred, but minor differences in the molybdenum and titanium contents might have been sufficient to alter the age-hardening characteristics and account for the scatter observed. The four E series tests performed in air were conducted at loading rates in the range 7.7 to 920 psi$\sqrt{\text{in.}}$/min. K_{Ic} was not noticeably dependent on loading rate.

The EC tests were performed either under free-corrosion conditions or under hydrogen-charging conditions. The latter were achieved by coupling the specimen to zinc anodes (potential $\approx$ -1060 mV) or polarizing potentiostatically to -1100 mV. The various results have been compared by plotting K^*_{Ii}/K_{Ic} as a function of loading rate in Figure 9. The results of tests performed under hydrogen-charging conditions are seen to fall on a single curve: at the very highest loading rates used, K^*_{Ii} is seen to be approximately equal to K_{Ic}, but as the loading rate decreases to about 1500 psi$\sqrt{\text{in.}}$/min, K^*_{Ii} increases to values considerably higher than K_{Ic}, before dropping to low values once again, at lower loading rates. The results for free-corrosion tests show similar trends, but, in addition, some points fall on a curve which shows a continuous decrease in K^*_{Ii} with decreasing loading rate. Under

some conditions, therefore, it would appear that the steel is "stronger" when tested in salt solution than when tested in air. However, the explanation for this apparent anomaly undoubtedly lies in the fact that two different crack paths are possible. Metallographic examination showed that EC may occur either in the precrack plane or along a well-defined plane inclined at about 60 degrees to, and on either side of, the precrack plane. The latter has been termed 'type 2' cracking by Carter [4], whilst cracking in the plane of the precrack has been termed 'type 1'. Thus, in the early stages, at least, type 2 cracking would have the effect of blunting the sharp precrack and reducing the stress-concentration factor, which would result in a higher load being required for the onset of fast fracture. At the lower loading rates, the blunting effect may still be appreciable, but because the crack would have time to propagate further across the specimen, the load to cause terminal fracture would be increasingly lowered as the loading rate was decreased. Occasionally, a third type of cracking, termed 'type 3', occurred at 90 degrees to the precrack plane: after extensive metallography, it was clear that these cracks were of a purely mechanical nature and were following stringers of carbonitrides and inclusions in the rolling plane.

The type of EC leading to failure is marked next to each point in Figure 9. It will be observed that the free-corrosion curve, which shows a continuous decrease in K^*_{Ii} with decreasing loading rate, represents specimens which have broken by type 1 cracking. Type 2 EC, on the other hand, can be associated with curves containing a maximum. The loading rate at which blunting is a maximum will obviously depend on the rate at

which a type 2 crack initiates and propagates: the slower the rate of cracking, the lower this critical loading rate will be. In Figure 9, the curve for the hydrogen-charged specimens has its maximum at about 1060 psi$\sqrt{\text{in.}}$/min, as compared with 550 psi$\sqrt{\text{in.}}$/min under free-corrosion conditions; this, then, is strong evidence that EC occurs more quickly in the hydrogen-charged specimens. The greater EC susceptibility of specimens which are cathodically polarized is further illustrated by the much lower K^*_{Ii} values at loading rates below 30 psi$\sqrt{\text{in.}}$/min.

Above 10,000 psi$\sqrt{\text{in.}}$/min, where the time to failure is less than 8 min, corrosion processes appear to play no part in the failure of freely corroding specimens, and fracture is purely mechanical.

The results summarized in Figure 9 provide little reason for supposing that the 24-hr cathodic pretreatment at zero load, given to the B series specimens, had any effect on the K^*_{Ii} value determined subsequently. Nor does the heat-treatment oxide appear to affect the cracking process in a freely corroding specimen loaded at 10 psi$\sqrt{\text{in.}}$/min, because when the oxide was removed from the surface of another specimen, the time-to-failure, potential-time curve, and K^*_{Ii} value determined for this specimen were almost identical to those obtained for the similar oxide-coated specimen tested under the same conditions.

The importance of employing a suitable loading rate to obtain a meaningful measure of EC susceptibility is clearly shown in these results. Thus, it seems logical that the effect of other variables on K^*_{Ii} should be measured at a loading rate below 10 psi$\sqrt{\text{in.}}$/min, where K^*_{Ii} values can be

depended upon to be less than K_{Ic}.

Effect of Potential on K^*_{Ii} (Cantilever Tests)

On the basis of the results presented in the last section, it was considered reasonable to study the effect of electrochemical potential on K^*_{Ii} at a loading rate of 9.2 (±1.9) psi$\sqrt{\text{in.}}$/min.

The susceptibility to EC was found to be very sensitive to potential, as is illustrated in Figure 10. A high K^*_{Ii} value may be an indication of a high K_{ISCC} value, but it may also be a reflection of a long incubation period or a slow crack-propagation rate. The type of cracking is marked next to each point in Figure 10.

Most of the specimens were polarized potentiostatically to the desired potential, but one was coupled to an aluminum alloy 5083 sacrificial anode (average potential, -782 mV) and two were allowed to corrode freely without any potential control (average potential, -575 mV).

Figure 10 shows that, by polarizing the specimen to slightly more positive (noble) potentials, the susceptibility to cracking increases, whilst the converse is true when the specimen is polarized slightly in the active direction. Such behaviour was considered by some workers [9,10,11] to be evidence of cracking by a SCC mechanism, but recent investigations [12] have shown that HEC is also a possibility, because hydrolysis reactions occurring within the advancing crack may reduce the pH locally to a value which permits hydrogen ion reduction and subsequent hydrogen absorption. However, results are presented elsewhere [8] which suggest that in 18% Ni maraging steel, SCC is the operative mechanism at free-corrosion

potentials.

The maximum in the K^*_{Ii} versus potential curve occurred at -750 mV: under these conditions, susceptibility to EC was at a minimum and K^*_{Ii} lay in the range of K_{Ic} values for this series. Although the steel was very resistant to cracking at this potential, metallographic examination showed that some EC had occurred. At more active potentials, the sharp drop-off in K^*_{Ii} values with increasing cathodic polarization is undoubtedly due to the increasing propensity to HEC. Whereas at free-corrosion potentials the cathodic reaction occurring on the specimen surface is oxygen reduction, at these more active potentials the primary reaction changes to hydrogen ion reduction, and hydrogen is absorbed by the metal and causes embrittlement.

Because 18% Ni maraging steel has been used occasionally in the fabrication of specialized marine craft, it is important to consider the resistance to EC under the appropriate operating conditions. The foils structure of the Canadian FHE 400 hydrofoil craft, for instance, is made from this steel, and there is metallic continuity between the foils and the aluminum alloy 5083 hull with its protective zinc sacrificial-anodes. Since both the aluminum alloy and the zinc are anodic to the maraging steel, there is no doubt that the electrochemical potential of the steel is shifted to more active values. If laboratory tests on precracked cantilever specimens can reasonably be compared with this service condition, then the steel will be polarized to some potential between -780 mV and -1060 mV; Figure 10 shows that, for steel containing a pre-existing crack, HEC is a very serious threat at these potentials.

Constant-load Cantilever Tests

As well as the standard E_1 series specimens, a few E_2 series specimens were also used for the constant-load cantilever tests. The latter specimens were similar to those of the E_1 series, except that there were no notches machined on the sides of the specimens. However, the results summarized in Figure 11 show that the time-to-failure is insensitive to side-notching, at least in freely corroding specimens.

The crack type leading to failure is marked next to each point in Figure 11.

Although very few tests were performed on specimens polarized to -1100 mV, there was little doubt that K_{ISCC} at this potential was about 31 ksi$\sqrt{in.}$ This value is very close to the K^*_{Ii} value of 31.4 ksi$\sqrt{in.}$ obtained in the rising-load tests on the E_1 series steel (see Figure 10), and is not greatly different from the K^*_{Ii} value of 28 ksi$\sqrt{in.}$ obtained in the slowest loading rate tests on the zinc-coupled E series specimens (see Figure 9). This all points to a very rapid rate of cracking in hydrogen-charged specimens at stress intensities above K_{ISCC}. This is further indicated in Figure 11 by the much shorter failure times at -1100 mV, as compared with those experienced at the free-corrosion potential. Even though K_{ISCC} was not determined for freely-corroding specimens, it is apparent that it lies below 40 ksi$\sqrt{in.}$, a stress intensity far below the K^*_{Ii} values determined in the rising-load free-corrosion tests on the E_1 series steel (Figure 9), and not very different from the K_{Ii} values obtained under hydrogen-embrittling conditions. This is confirmation that higher K^*_{Ii} values do not necessarily

result from a higher K_{ISCC}; and Figure 12 demonstrates that, under free-corrosion conditions, both the rate of cracking and the incubation period differ considerably from those experienced in specimens polarized to -1100 mV. The beam-deflection vs time curves in Figure 12 reflect the progress of EC under both sets of conditions. Even though the initial stress intensity for the freely corroding specimen was over twice that for the hydrogen-charged specimen, the rate of EC is seen to be lower under free-corrosion conditions; also,the absence of an incubation period at -1100 mV contrasts with the initial 90-min period of constant beam-deflection for the free-corrosion specimen. Even when K_{Ii} was only slightly higher than K_{ISCC}, there was never any suggestion of an incubation period at -1100 mV, and slow crack growth always commenced immediately. In freely corroding specimens, the incubation period ranged from 0.6 hr at high K_{Ii} values to a few days at low K_{Ii} values.

Unisteel Tests

Table 4 gives the 0.2% offset yield strength for the B_u and D_u series parent-metal specimens, and for the C_u and D_u series weld-metal specimens, as determined using a standard tensile testing technique.

Both weld-metal and parent-metal specimens were loaded at 85 to 90% of their yield strength, and either were allowed to corrode freely or were coupled to zinc. The results are summarized in Figure 13, where groups of data points have been bracketed, each of the three bracketed groups corresponding to a particular set of test conditions. The data point for one zinc-coupled parent-metal specimen (time to failure, 1584 hr) has

been excluded from the "cathodic protection" bracket, because, as will be discussed below, it is not typical of that group. It can be seen that freely corroding parent-metal specimens, had, on average, about twice the life of the weld-metal specimens. Furthermore, the failure times of both types of specimen were greatly increased when they were cathodically protected by coupling to zinc. Such behaviour, of course, is in direct contrast to that observed in the cantilever tests, where polarizing to the zinc potential was undoubtedly deleterious. The extended life of the zinc-coupled Unisteel specimens resulted because cathodic polarization of the specimen effectively suppressed pit formation. Thus, neither precracks nor pits were available to provide the local stress concentration necessary to promote hydrogen segregation in such areas, and subsequent HEC.

In fact, an examination of the six cathodically protected specimens showed that definite corrosion had occurred in three of them, including the two which had failed in times of 1584 hr and 2248 hr. In these three specimens, corroded connections resulted in the loss of cathodic protection over part of the testing period; had it been maintained, presumably none of the specimens would have cracked within the chosen test period of 2400 hr (100 days). The two specimens which did fail both did so without any appreciable necking occurring in the gauge length.

Of all the freely corroding specimens, only two weld-metal specimens and one parent-metal specimen fractured without noticeable necking in the gauge length. The other nine specimens appeared to have failed primarily because general corrosion and pitting had reduced the cross section sufficiently

at some point to allow local necking, followed by intensified corrosion in this region. It is quite possible that EC could have played some role in the failure of these necked specimens, but there is no doubt that EC occurred in the three specimens which showed no necking. In the latter specimens, it is likely that a fairly narrow pit formed and promoted EC from its base: because the environmental cracks were themselves fairly sharp, very little penetration would be necessary before the stress intensity at the crack tip would reach the critical value for purely mechanical fast fracture.

Figure 14 shows two of the B_u series (parent metal) fractures: one which failed with and one which failed without necking.

DISCUSSION

The results of the Unisteel tests showed that polarizing 18% Ni maraging steel to zinc potentials can be beneficial if smooth specimens are used; this observation is consistent with that of other workers [13, 14] who used smooth specimens. However, it is realistic to assume that in a complex structure fabricated from maraging steel (e.g., a hydrofoil), a small crack, or some other surface defect which might serve as a stress-raiser, will pre-exist or will form during service. Thus the results obtained with precracked cantilever specimens are undoubtedly more characteristic of the behaviour to be expected under most service conditions. The Unisteel test has one further disadvantage: at the high applied stresses needed to give failures in reasonable testing periods, very little general corrosion or

pitting is required to promote necking and subsequent fracture by overloading. For instance, if a standard Unisteel specimen were loaded to 90% of the yield strength, necking would begin to take place if uniform general corrosion were to reduce the radius of the gauge length by 0.0032 in. It is possible that failure of a specimen could occur without EC ever playing a role.

There were no definite indications of weld defects in the Unisteel specimens used for this work but, had they been present, the results might have been very different. Imperfect weld-metal penetration, for instance, would give rise to a flaw which could perform the same function as a precrack. This suggestion may explain why some workers [14] found that their smooth weld-metal specimens of maraging steel failed in relatively short times.

On the basis of the results reported above, it is suggested that the rising-load cantilever test gives a rapid evaluation of the EC properties of a high-strength material, in terms of the nominal stress intensity, K^*_{Ii}. It has been demonstrated that, for 18% Ni maraging steel, a suitable loading rate would be 10 psi$\sqrt{\text{in.}}$/min or less; in order to minimize testing time a rate in the range 5-10 psi$\sqrt{\text{in.}}$/min would be appropriate, this being equivalent to a 0.5-1 week testing period for the specimens used in this work. Though not reported here in detail, some preliminary tests on HY 140 [15] and 12% Ni maraging steels also show that a loading rate of 5-10 psi$\sqrt{\text{in.}}$/min is quite suitable. Using this method, the comparative susceptibilities of various high-strength materials to EC can be determined with only two or

three specimens of each material. Or, if the EC susceptibility of a single material in various corrodents or at various potentials is required, determination of K^*_{Ii} will give a combined measure of incubation time, crack propagation rate, and K_{ISCC}. All three parameters are important, but the single quantity, K^*_{Ii}, takes into account the relative importance of each and gives an overall measure of EC susceptibility.

When different materials are compared, due account must, of course, be given to possible differences in K_{Ic}. In instances where different heats of the same material are compared, there is merit in presenting the results in the form K^*_{Ii}/K_{Ic}, as shown in Figure 9.

Figure 10 illustrates how the rising-load cantilever test can be usefully employed to determine the best cathodic protection system for 18% Ni maraging steel. Clearly, when complex structures such as the Canadian FHE-400 hydrofoil craft are cathodically protected at or near zinc potentials (about -1060 mV), there is a serious danger of failure by HEC. Because there appears to be no EC incubation period at such potentials, and crack-propagation rates are high, failure could occur quite rapidly. Cathodic protection by zinc should, therefore, be avoided.

The highest K^*_{Ii} value, and the highest resistance to EC, occurred at a potential of about -750 mV: this potential might in some instances be achieved by coupling the steel to sacrificial anodes of cadmium, or perhaps by coating the whole surface with cadmium. Though this would give best protection theoretically, the sharp deterioration in properties at the nearby potential of -780 mV might warrant the choosing of some slightly more noble

potential, e.g., in the vicinity of -700 mV as optimum. Of course, in some service applications, devising practical methods of holding structures in the narrow potential range giving maximum resistance to EC would constitute an extremely difficult problem.

ACKNOWLEDGEMENT

The authors would like to thank J.G. Garrison for his help with the experimental work.

REFERENCES

1. B.F. Brown, Met. Rev. 13, 171 (1968).
2. H.R. Smith, D.E. Piper and F.K. Downey, "A Study of Stress-Corrosion Cracking by Wedge-Force Loading", Boeing Document D6-19768 (1967), Renton, Washington.
3. B.F. Brown and C.D. Beachem, Corr. Sci. 5, 745 (1965).
4. C.S. Carter, "Crack Extension in Several High-Strength Steels Loaded in 3.5% Sodium Chloride Solution", Boeing Document D6-19770 (1967), Renton, Washington.
5. G.J. Biefer and J.G. Garrison, "Stress Corrosion Cracking Tests on Some High-Strength Steels, Using the USNRL Cantilever Method", Mines Branch Technical Bulletin TB 114, Department of Energy, Mines and Resources, Ottawa, Canada (1969).

6. C.N. Freed and J.M. Krafft, J. Materials 1, 770 (1966).

7. "Proposed Method of Test for Plane-Strain Fracture Toughness of Metallic Materials", ASTM Standards, Part 31, 1099 (May 1969).

8. B.C. Syrett, "Environmental Cracking in 18% Ni Maraging Steel", submitted for publication in Corrosion (1970).

9. P.C. Hughes, J. Iron and Steel Inst. 204, 385 (1966).

10. R.N. Parkins and E.G. Haney, Trans. AIME 242, 1943 (1968).

11. B.F. Brown, Report of NRL Progress (May 1958).

12. B.F. Brown, "On the Electrochemistry of Stress-Corrosion Cracking of High Strength Steels", presented at the Fourth International Congress on Metallic Corrosion, Amsterdam, Netherlands (1969).

13. W.W. Kirk, R.A. Covert and T.P. May, Metals Eng. Quarterly 8, 31 (1968).

14. R.D. Barer, "Stress Corrosion and Corrosion Fatigue Behaviour of 250 kpsi Maraging Steel in Sea Water", Pacific Naval Laboratory Materials Report 66-C, Esquimalt, British Columbia (1966).

15. G.J. Biefer and B.C. Syrett, "Environmental Cracking Test on High Strength Steels Using the U.S.N. Cantilever Test", presented at the Third Inter-Naval Corrosion Conference, London, England (1969).

▪ = = =

BCS:GJB:(PES)1m

TABLE 1

General Description of the 18% Ni (250) Maraging Steels

Source (all series)	:	Vanadium-Alloys Steel Co.
As-received condition (all series)	:	Consumable arc, vacuum-melted, 0.5-in. plate in the solution-annealed condition.
Additional heat treatment (all series)	:	3 hr at 482°C (900°F), air cooled

Series B, C_1, E, E_1 and E_2 were cantilever tests; only E_2 series specimens were machined without the side-notches shown in Figure 1.

Series B_u, C_u and D_u were "Unisteel" tests.

Final thickness of cantilever specimens after machining:

B series, 0.501 in.; C_1 series, 0.440 in.;
E series, 0.502 in.; E_1 series, 0.500 in.;
E_2 series, 0.482 in.

TABLE 2

Chemical Composition* of the Maraging Steels

Series	C	Si	Mn	S	P	Al	Ti	B	Mo	Co	Ni	Zr	Ca
B, B_u	0.015	0.03	0.04	0.008	0.004	0.06	0.39	0.003	4.45	7.97	19.20	0.01	0.004
C_1, C_u	0.017	0.04	0.04	0.008	0.004	0.06	0.38	0.003	4.58	7.50	18.78	0.01	0.005
E, E_1, E_2	0.018	0.04	0.04	0.008	0.004	0.06	0.40	0.003	4.46	7.92	19.22	0.01	0.003

* Analysis at the Department of Energy, Mines and Resources, Ottawa.

TABLE 3

Fracture Toughness of the Maraging Steels

Series	B	C_1	E	E_1, E_2
No. of specimens tested	1	2	4	2
K_{Ic}, ksi$\sqrt{in}$.	78.7	69.9 ± 0.5	95.5 ± 7.0	87.7 ± 1.9

TABLE 4

0.2% Offset Yield Strength of the Maraging Steels

Series	Weld or Parent Metal	0.2% Offset Yield Strength (ksi)
B_u	Parent	241
C_u	Weld	237.5
D_u	Parent	240
D_u	Weld	203

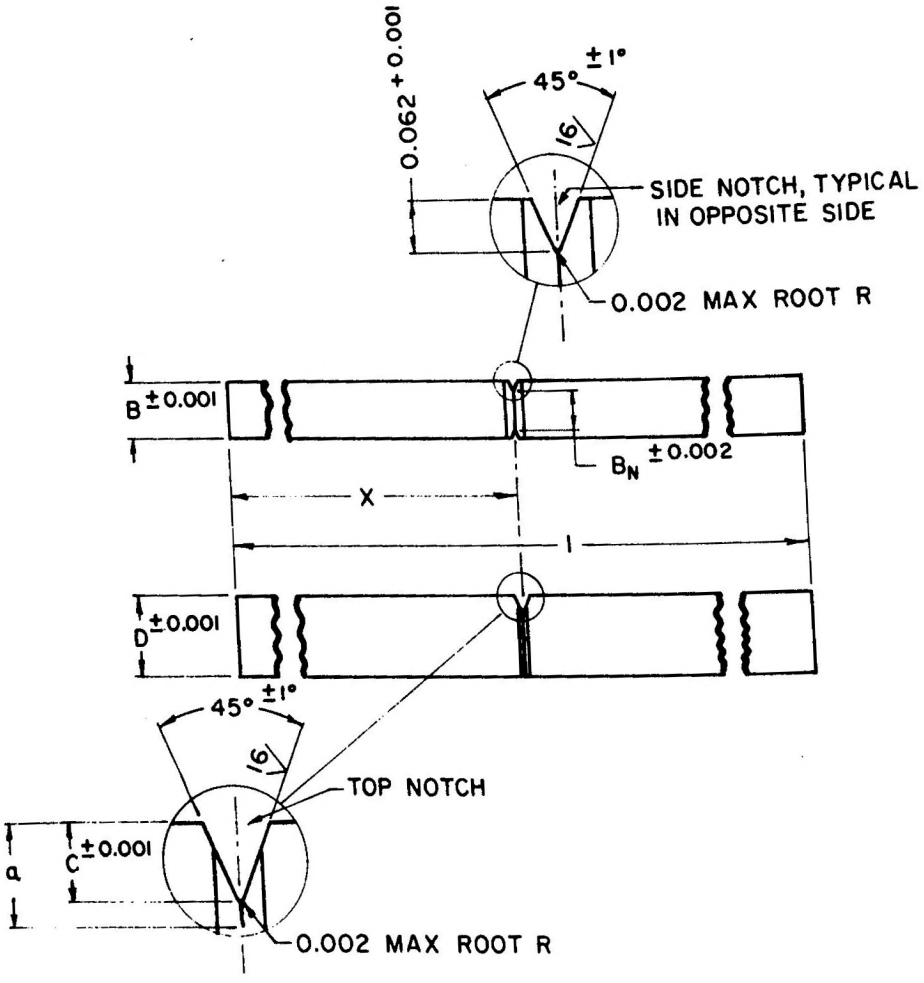

X = 3.0 - 3.2 in.
I = 6.0 - 6.4 in.
D = 0.440 - 0.502 in. = specimen depth.
B = 0.375 in. = specimen thickness.
B_N = 0.250 in. = specimen thickness in plane of notches.
C = 0.113 in. = notch depth.
a = notch depth plus fatigue crack depth.

Figure 1. Dimensions of Standard Cantilever Test Specimen.

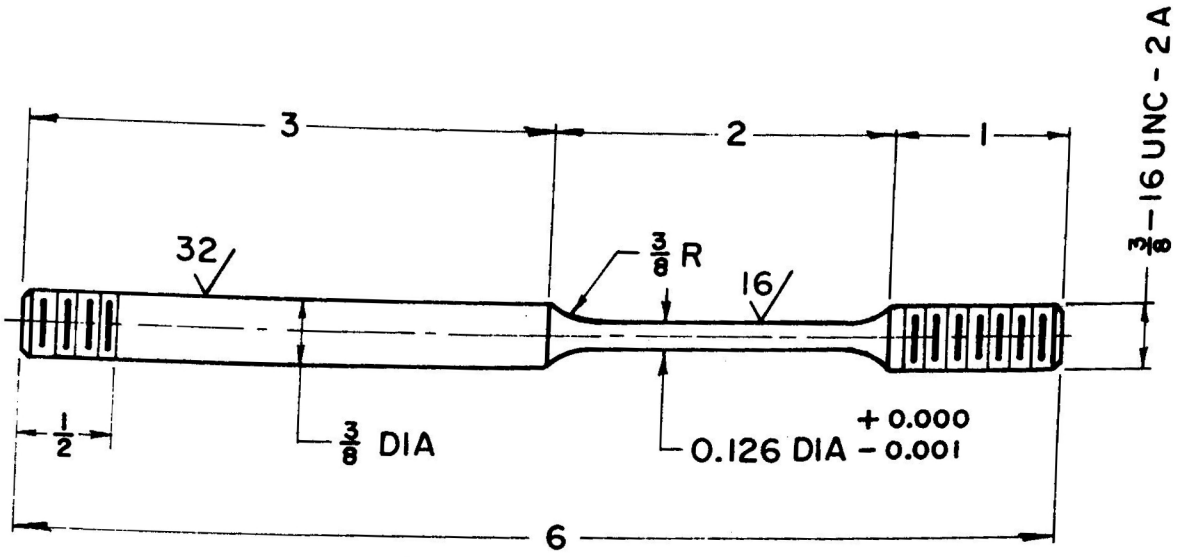

Dimensions in Inches

Figure 2. Dimensions of the Unisteel Specimens.

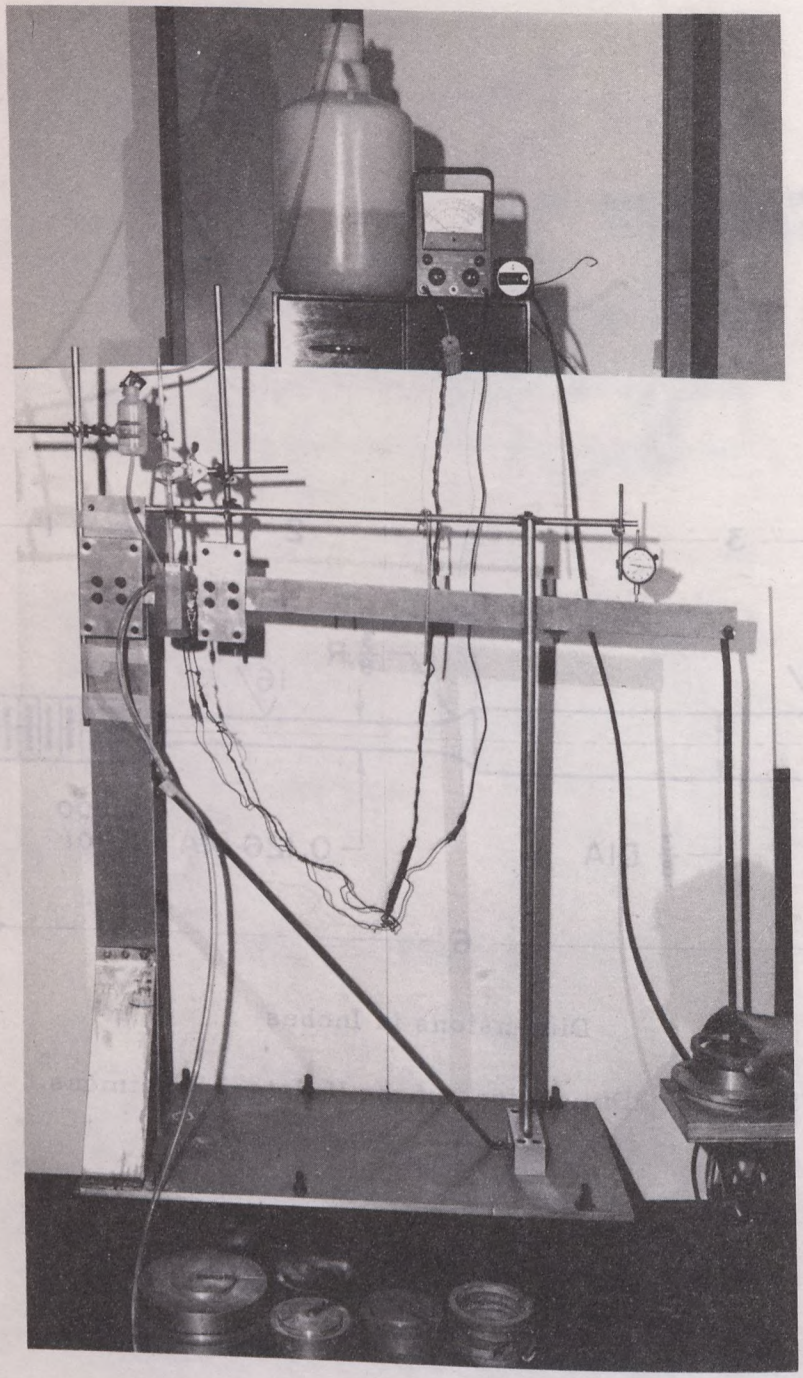

Figure 3. Manually-Loaded Cantilever Testing Rig.

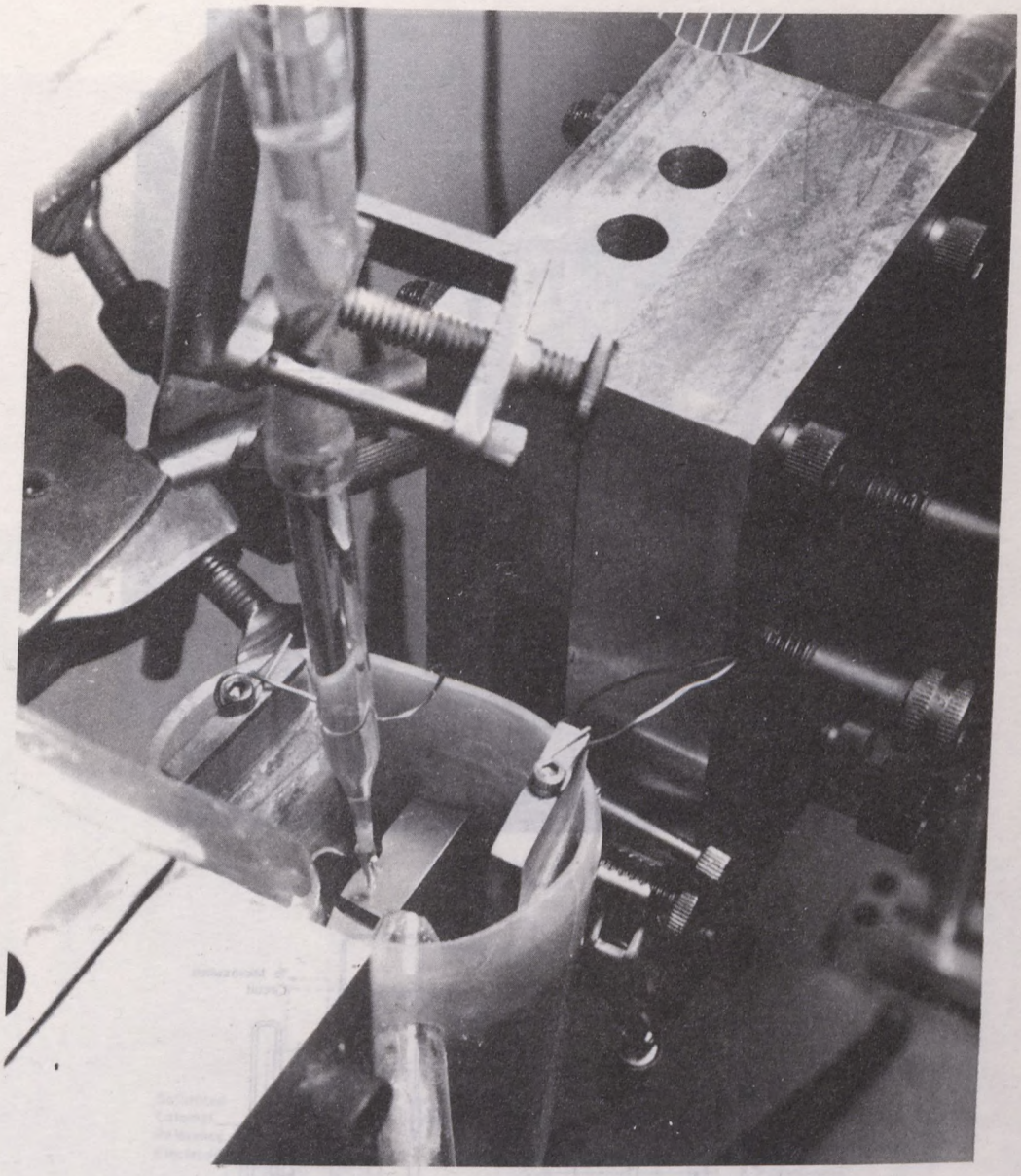

Figure 4. The Corrosion Cell and Notched Specimen in the Manually-Loaded Cantilever Testing Rig. The specimen is shown under "cathodic protection" by sacrificial anodes.

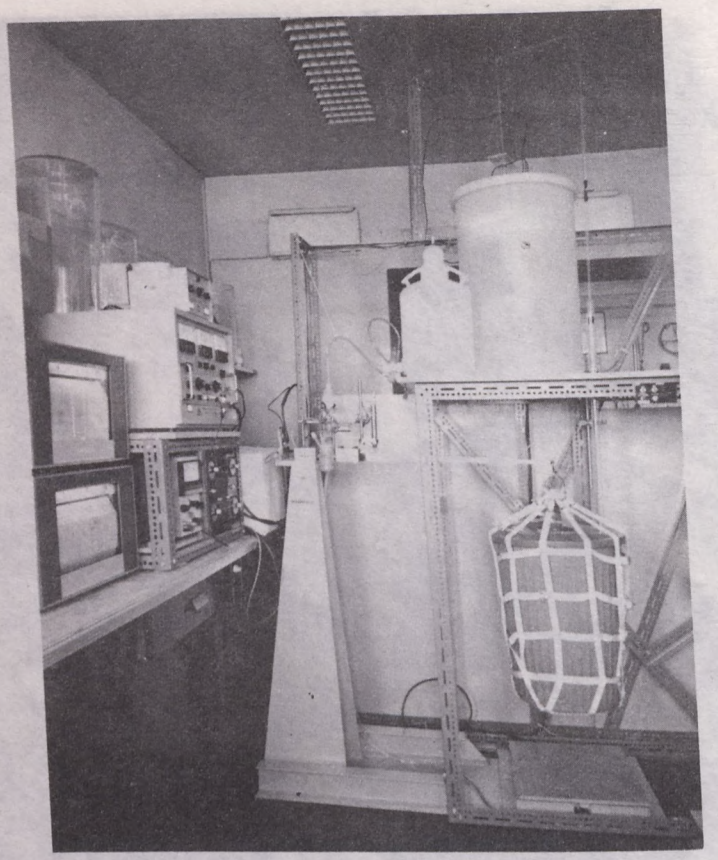

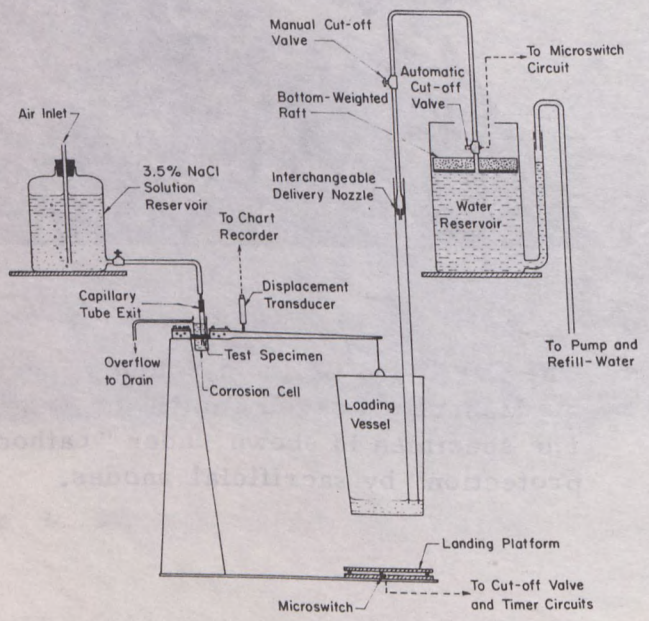

Figure 5. Automated Cantilever Testing Rig.

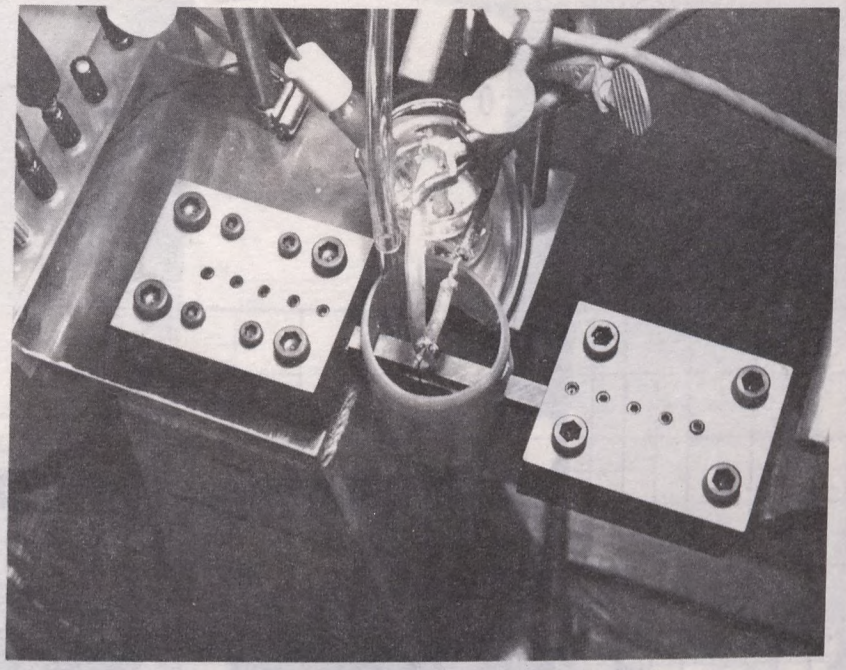

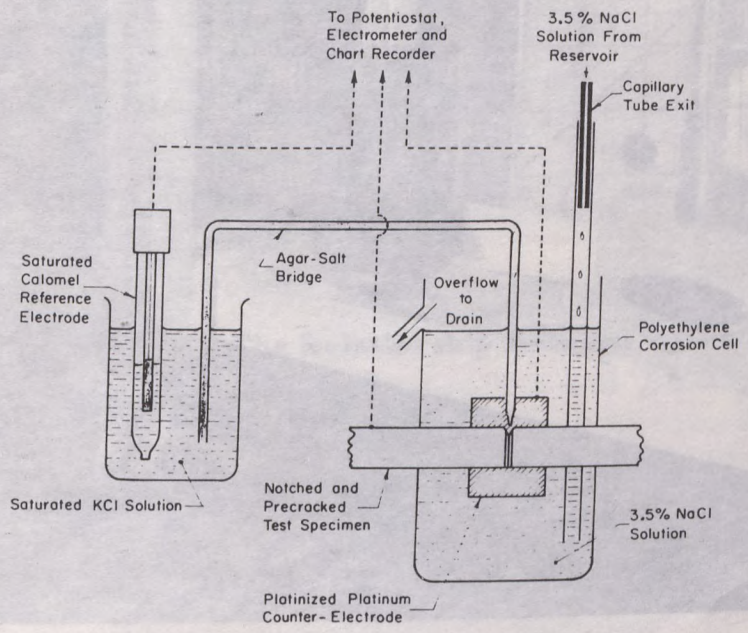

Figure 6. Cantilever Test Specimen and Corrosion Cell of Automated Rig.

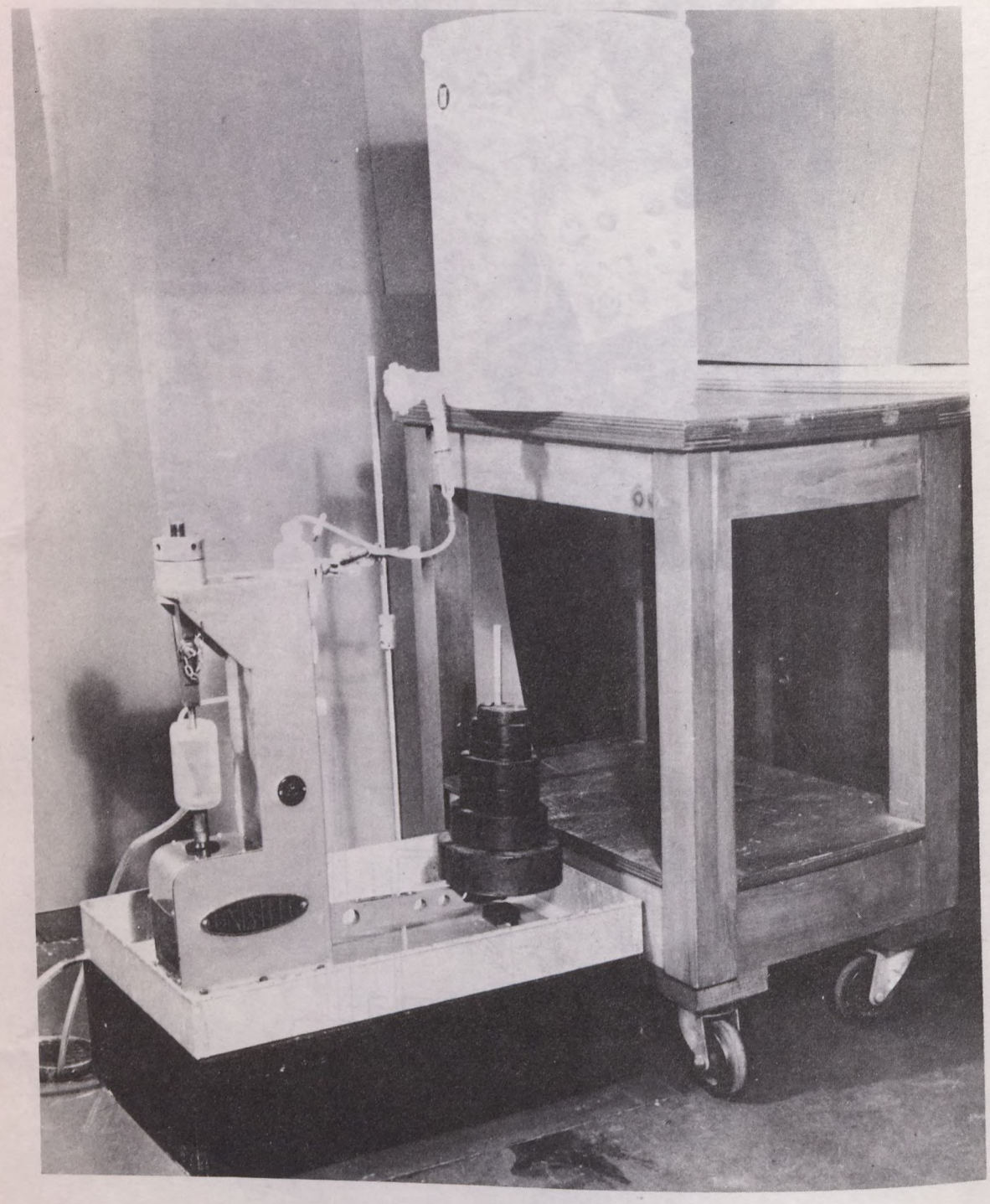

Figure 7. The Unisteel Testing Machine.

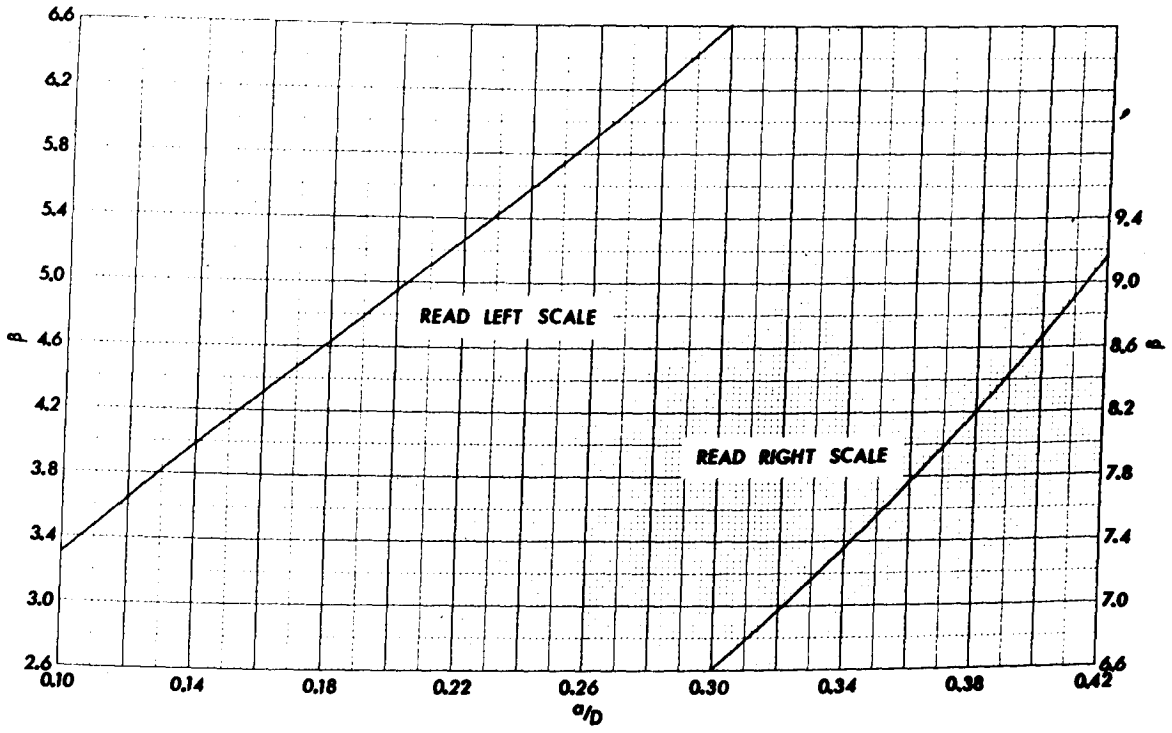

Figure 8. The Relationship Between α/D and β.

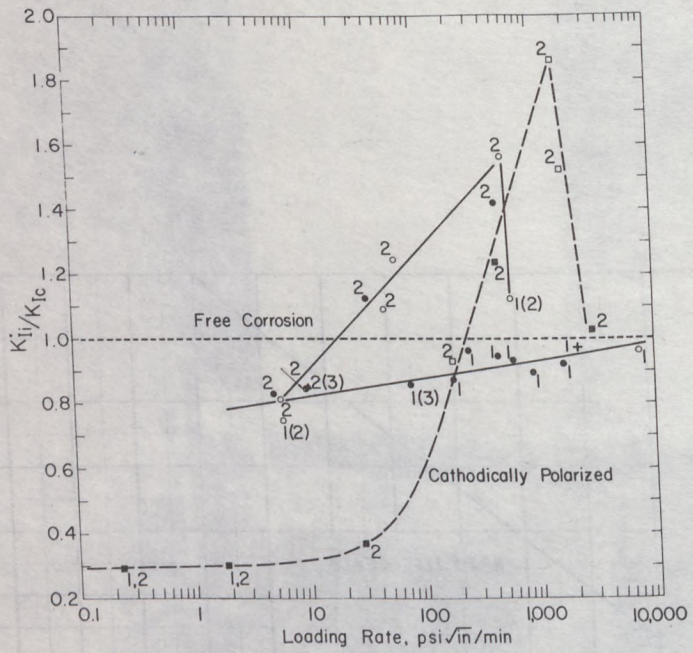

□ B Series, polarized potentiostatically to -1100 mV during test and for 24 h. prior to testing (K_{Ic} = 78.7 ksi$\sqrt{in.}$)

■ E Series, polarized to about -1060 mV during test by coupling to zinc (K_{Ic} = 95.5 ± 7.0 ksi$\sqrt{in.}$)

o C_1 Series, free corrosion (K_{Ic} = 69.9 ± 0.5 ksi$\sqrt{in.}$).

\+ C_1 Series, free corrosion for 100 h. at zero load followed by drying and fracture in air.

• E_1 Series, free corrosion (K_{Ic} = 87.7 ± 1.9 ksi$\sqrt{in.}$).

▲ E_1 Series, free corrosion: heat treatment oxide removed prior to testing.

Figure 9. Effect of Loading Rate on K^*_{Ii} for (a) Freely Corroding Specimens, (b) Cathodically Protected Specimens.

[Free-corrosion data from Reference 8].

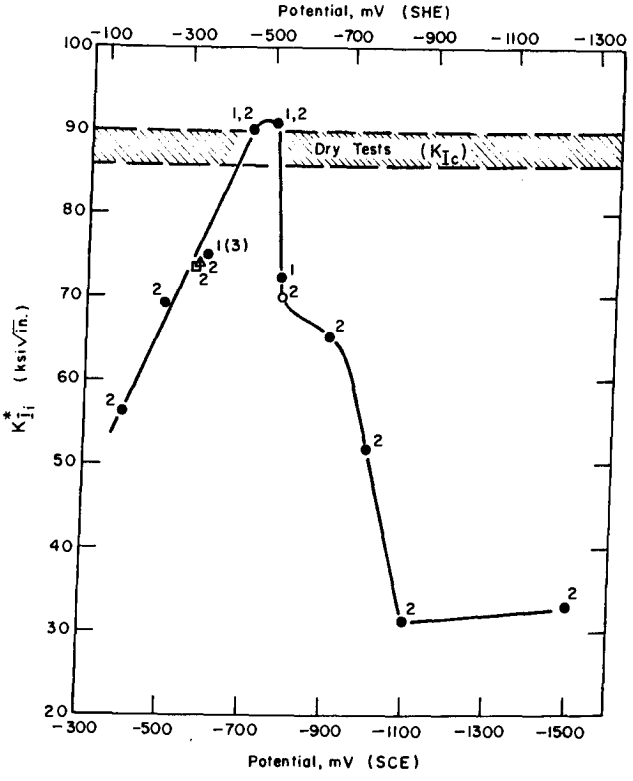

- • Potential controlled by a potentiostat.
- o Specimen coupled to aluminum alloy 5083.
- □ Free corrosion.
- Δ Free corrosion, heat treatment oxide removed prior to testing.

1, 2, 3. Respectively types 1, 2 and 3 cracking over most of the crack front. Brackets around a number signify this type of cracking over a small section of the crack front.

Figure 10. Effect of Potential on the K^*_{Ii} Values. [After Syrett (8)].

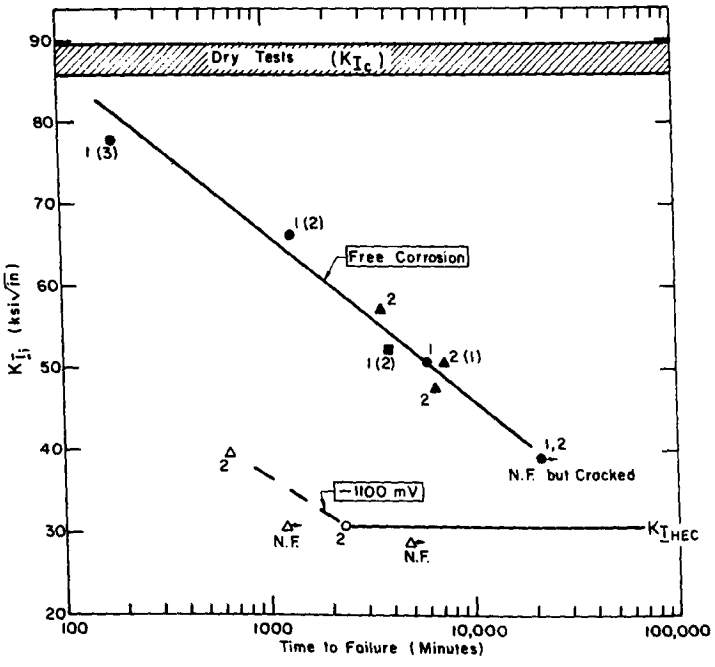

● ■ ▲ Free corrosion. o Δ Polarized to -1100 mV.

● o Standard specimens (E_1 series) in 3.5% NaCl solution.

▲ Δ Specimens without side-notches (E_2 series) in 3.5% NaCl solution.

■ Specimen without side-notches (E_2 series) in 3.5% NaCl solution containing 4 mg/litre $NaAsO_2$.

N.F. No failure during time indicated.

1, 2, 3. Respectively types 1, 2 and 3 cracking over most of the crack front. Brackets around a number signify this type of cracking over a small section of the crack front.

Figure 11. The Effect of K_{Ii} on the Time to Failure Under (a) Free-Corrosion Conditions, (b) Hydrogen Charging Conditions (Polarized to -1100 mV). [After Syrett (8)].

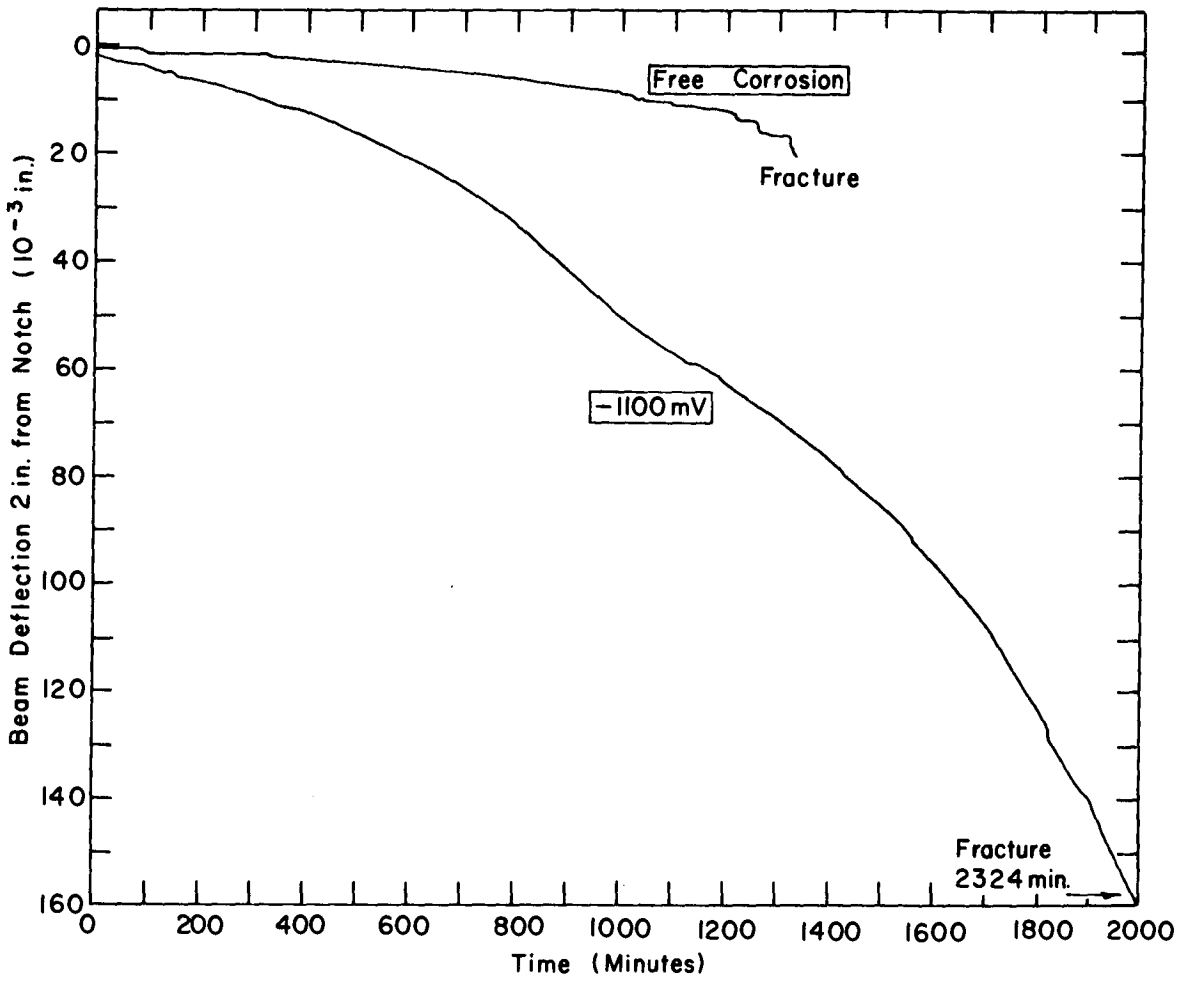

Figure 12. Beam Deflection-Time Curves for Cantilever Specimens Tested at Constant Load Under (a) Free-Corrosion Conditions (K_{Ii} = 66.3 ksi$\sqrt{in.}$), and (b) Hydrogen Charging Conditions (-1100 mV; K_{Ii} = 30.9 ksi$\sqrt{in.}$). [After Syrett (8)].

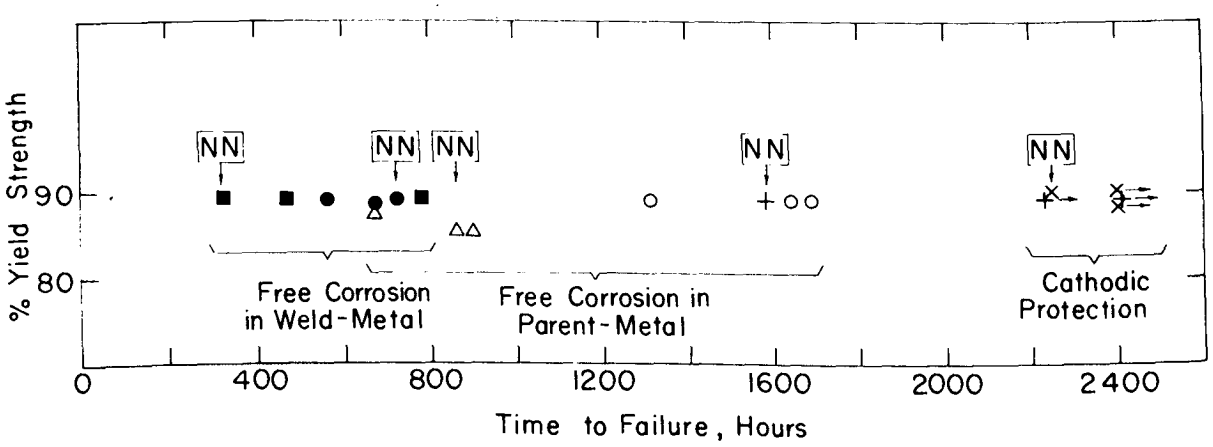

Δ B_u series (parent). Free corrosion.
■ C_u series (weld). Free corrosion.
o D_u series (parent). Free corrosion.
● D_u series (weld). Free corrosion.
\+ D_u series (parent). Coupled to Zn.
× D_u series (weld). Coupled to Zn.
→ No failure in time indicated.
NN Specimen failed without necking.

Figure 13. Time to Failure of Unisteel Specimens Stressed at 85 to 90% of the Yield Strength in 3.5% NaCl Solution.

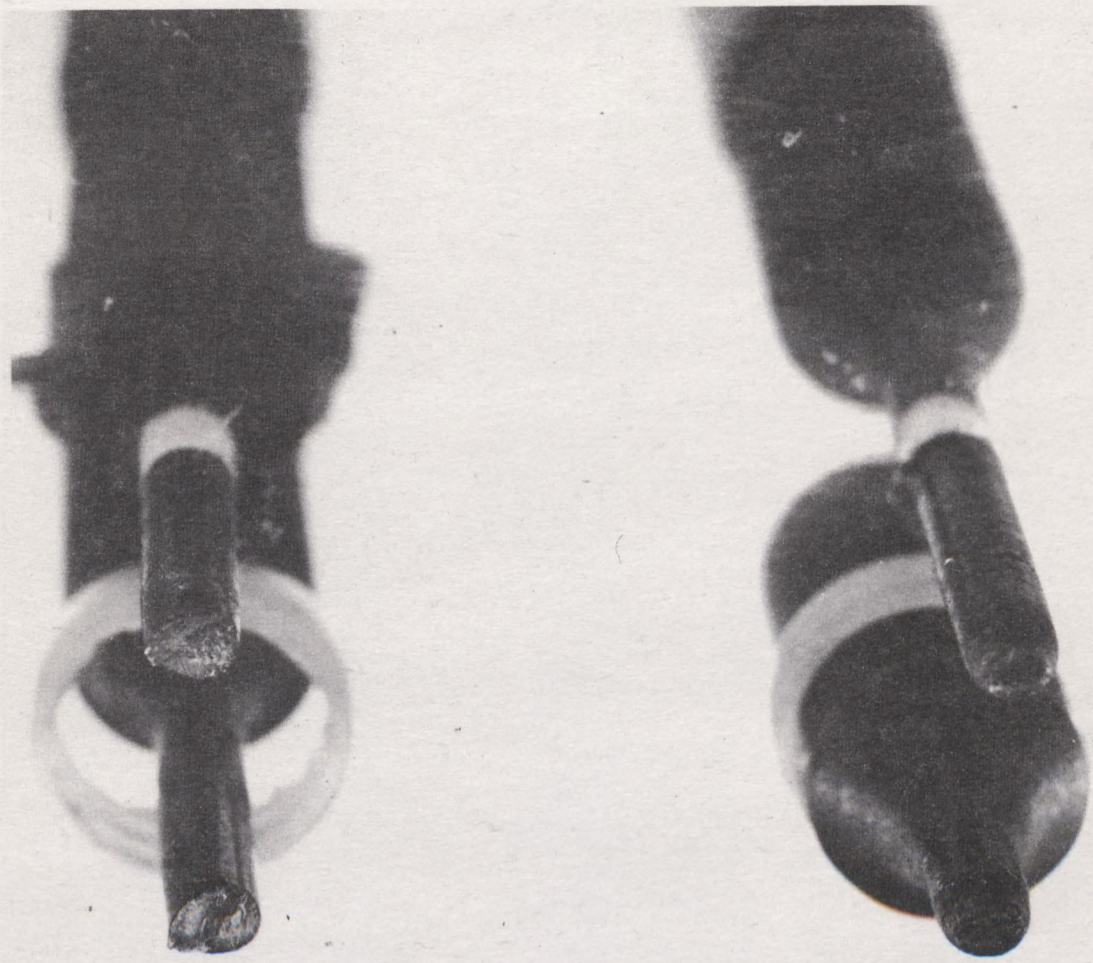

(a)
Without Necking

(b)
With Necking

Figure 14. Two B_u Series (Parent-Metal) Specimens: One Failing Without and One With Necking.

DEPARTMENT OF ENERGY, MINES AND RESOURCES

GEOLOGICAL SURVEY OF CANADA MINES BRANCH

LEGEND

MAP

Bedding attitude

Contraction fault attitude

Slip linear on bedding

Slip linear on contraction fault

*Thrust fault, teeth on upthrust side

*Diabase dyke

*Steeply dipping fracture with slip linears

A B Domain boundary

3 Location of elastic strain recovery measurements in vertical holes

-600 Contours on hangingwall of orebody, elevation below shaft collar

*Note: Horizontal projection of the intersection with the hangingwall of the orebody

n 5 10% Rose Diagram - strike frequency of smooth joints (n number of measurements).

FABRIC DIAGRAMS

Pole to bedding

Pole to contraction fault

Pole to diabase dyke or sill

Pole to fracture with slip linears

Slip linears, arrow indicates sense of displacement of hangingwall block

Compiled and drawn by H. U. Bielenstein, 1969

Prepared for publication by the Geological Cartography Unit

To accompany Mines Branch Research Report R 210

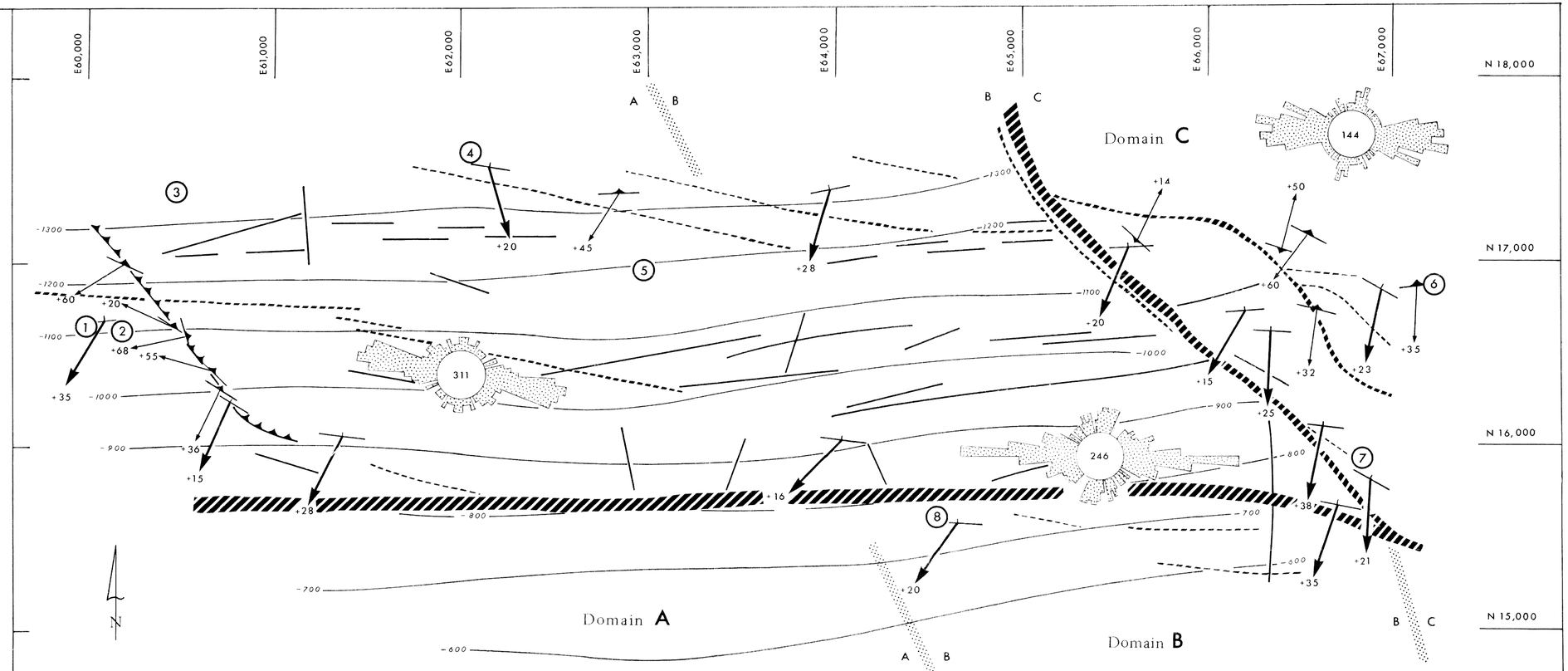

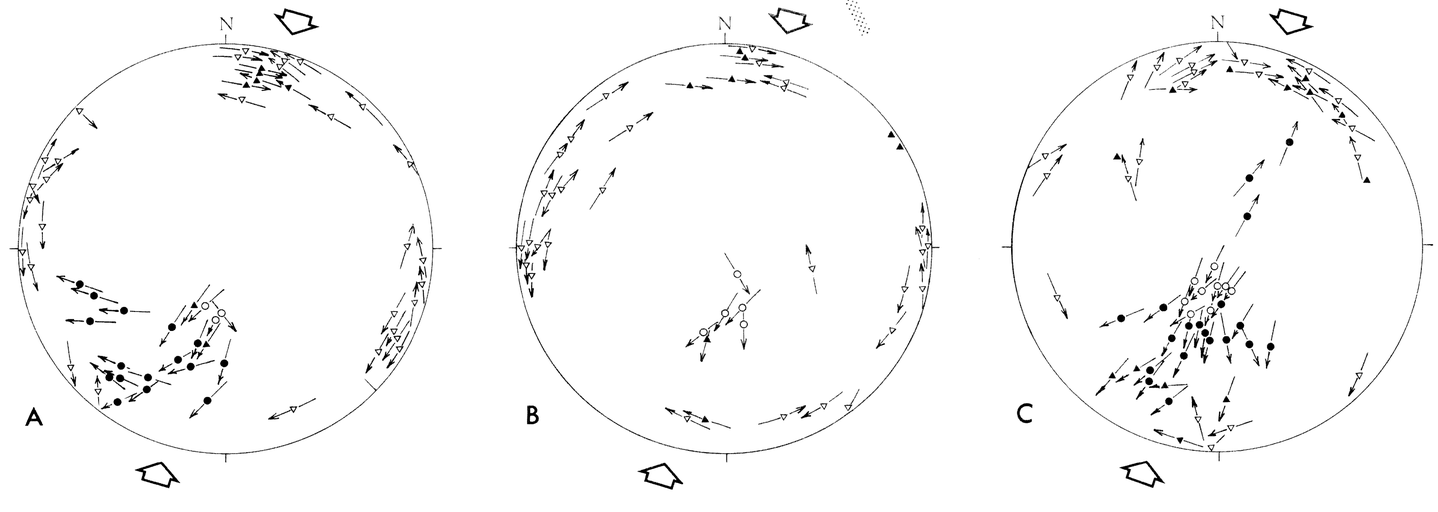

Figure 14.

Tectonic map of Rio Algom Nordic Mine, Ontario.

SCALE

500 0 500 1000

feet

Published, 1970

Printed by the Surveys and Mapping Branch

DEPARTMENT OF ENERGY, MINES AND RESOURCES

GEOLOGICAL SURVEY OF CANADA MINES BRANCH

83°00' 45' 82°30' 46°30' 46°15'

LEGEND TO KINEMATIC MAP

- Cutler granite and metamorphic Proterozoic sedimentary and igneous rocks
- Nipissing diabase
- Cobalt group
- Pre-Cobalt (Elliot Lake Gr., Hough Lake Gr., Quirke Lake Gr.) — Proterozoic sedimentary rocks (Huronian)
- Granite
- Greenstone-Greywacke — Archean
- Bedding and Bedding-Plane Slip Linear
- Slaty cleavage
- Flexural-flow folds (a rotational axis with vergence looking down the plunge)
- Thrust faults
- Strike-slip faults

Boulder-matrix slip linear

Fractures in boulders

Slip linears on fractures in granite

G. M. Eisbacher

Compiled and drawn by ~~H. U. Bielenstein~~, 1969

Prepared for publication by the Geological Cartography Unit

To accompany Mines Branch Research Report R 210

FLACK LAKE FAULT

TEN MILE LAKE FAULT

QUIRKE LAKE FAULT

SPANISH AMERICAN FAULT

MOON LAKE FAULT

GULLBREAK LAKE FAULT

HORNE LAKE FAULT

PECORS LAKE FAULT

HOUGH LAKE FAULT

BATTY LAKE FAULT

NORDIC MINE

LAKE OF THE MOUNTAIN FAULT

MURRAY FAULT

WHALESBACK CHANNEL

INDIAN RESERVE

Published, 1970

Printed by the Surveys and Mapping Branch

MAP 1

KINEMATIC MAP OF THE ELLIOT LAKE REGION

0 1 2 3

MILES

DEPARTMENT OF ENERGY, MINES AND RESOURCES

GEOLOGICAL SURVEY OF CANADA MINES BRANCH

83°00' 45' 82°30' 46°30' 46°15'

LEGEND TO DYNAMIC MAP

Cutler granite and metamorphic Proterozoic sedimentary audigneous rocks

Proterozoic sedimentary rocks and diabase

Granite

Greenstone-Greywacke } Archean

Smooth joint

Group of smooth joints

Fracture trend from air photographs

BM Compression axis from boulder-matrix slip

C Compression axis from conjugate contraction faults

G

Statistical presentation of compression axes derived from slip linears on fractures in granite (contour interval 2 standard deviations, Kamb, 1959).

Schmidt equal-area diagram of late quartz veins, presented as generalized great circle sections.

G. H. Fisher

Compiled and drawn by ~~H. U. Bielenstein~~, 1969

Prepared for publication by the Geological Cartography Unit

To accompany Mines Branch Research Report R 210

NORDIC MINE

INDIAN RESERVE

WHALESBACK CHANNEL

Published, 1970

Printed by the Surveys and Mapping Branch

MAP 2

DYNAMIC MAP OF THE ELLIOT LAKE REGION

0 1 2 3

MILES